Journal of Advanced Research 9 (2018) 69–77

Contents lists available at ScienceDirect

Journal of Advanced Research

journal homepage: www.elsevier.com/locate/jare

Original Article

Synthesis and characterization of ZnO phytonanocomposite using *Strychnos nux-vomica* L. (Loganiaceae) and antimicrobial activity against multidrug-resistant bacterial strains from diabetic foot ulcer

Katherin Steffy [a,*], G. Shanthi [a], Anson S. Maroky [b], S. Selvakumar [c]

[a] Division of Microbiology, Rajah Muthiah Medical College, Annamalai University, Chidambaram 608002, Tamil Nadu, India
[b] Department of Pharmacy, Faculty of Engineering and Technology, Annamalai University, Chidambaram 608002, Tamil Nadu, India
[c] Department of Zoology, Faculty of Science, Annamalai University, Chidambaram 608002, Tamil Nadu, India

GRAPHICAL ABSTRACT

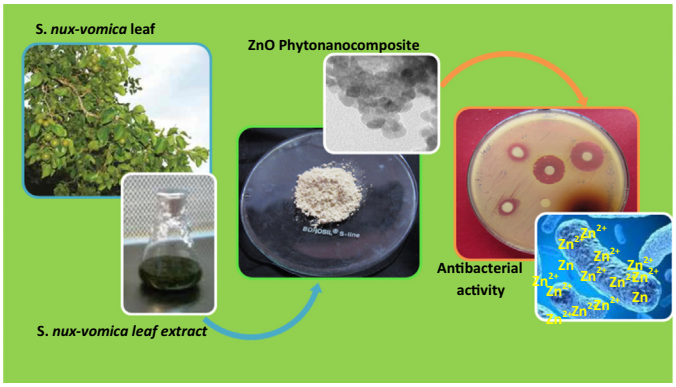

ARTICLE INFO

Article history:
Received 18 June 2017
Revised 25 October 2017
Accepted 2 November 2017
Available online 3 November 2017

Keywords:
ZnO phytonanocomposite
Strychnos nux-vomica
Multidrug resistance (MDR)
Antibacterial activity

ABSTRACT

Nanobiotechnology has been emerged as an efficient technology for the development of antimicrobial nanoparticles through an eco-friendly approach. In this study, green synthesized phytonanocomposite of ZnO from *Strychnos nux-vomica* leaf aqueous extract was characterized by X-ray diffraction analysis (XRD), UV–visible-spectroscopy, Photoluminescence spectroscopy (PL), Fourier transform infrared spectroscopy (FTIR), X-ray photoelectron spectroscopy (XPS), High-resolution Transmission Electron Microscopy (HR-TEM), and Energy dispersive X-ray analysis (EDX). Antibacterial activity was investigated against multidrug-resistant bacteria (MDR) isolated from diabetic foot ulcers (DFUs), such as MDR–methicillin resistant *Staphylococcus aureus* (MRSA), MDR–*Escherichia coli,* MDR–*Pseudomonas aeruginosa,* MDR–*Acinetobacter baumannii,* as well as against standard bacterial strains, *S. aureus* ATCC 29213, *E. coli* ATCC 25922, *P. aeruginosa* ATCC 27853, and *E. faecalis* ATCC 29212 through disc diffusion assays on Muller Hinton Agar. The characterization studies revealed a size-controlled synthesis of quasi-spherical hexagonal wurtzite structured ZnO phytonanocomposite with an average size of 15.52 nm. Additionally, remarkable bactericidal activities against MDR clinical as well as ATCC bacterial strains were exhibited, with a maximum zone of inhibition of 22.33 ± 1.53 mm (against *S. aureus* ATCC 29213) and 22.33 ± 1.16 mm (MDR–MRSA) at a concentration of 400 μg/mL. This study thus established the

Peer review under responsibility of Cairo University.
* Corresponding author.
E-mail addresses: katherinsteffy88@gmail.com (K. Steffy), drgshanthi@yahoo.com (G. Shanthi), ansonmarokey@gmail.com (A.S. Maroky), drsselvakumarau@gmail.com (S. Selvakumar).

https://doi.org/10.1016/j.jare.2017.11.001

possibility of developing antimicrobial ZnO nanocomposite of *Strychnos nux-vomica* leaf extract to combat developing drug resistance currently being experienced in health care facilities.

Introduction

Nanotechnology is a rapidly growing branch in the field of Science and Engineering that uses the design of novel state-of-the-art tools in both diagnostics and therapeutics due to inimitable properties of nanomaterials. Among inorganic metals, the unique physicochemical properties of ZnO make it a feasible and exceptionally attractive compound applicable for a variety of nanotechnology applications [1]. The synthesis of variable ZnO nanostructures can be carried out meticulously with great control due to the following features: (i) photonic and piezoelectric properties, (ii) stable polar surface and inimitable chemical qualities of simple crystal-growth technology [2,3], (iii) IEP range within 1.7–3.5 [4], and (iv) high excitonic binding energy of 60 meV [5]. ZnO nanostructures also exhibit significant antibacterial and antifungal properties [6]. Selective toxicity of ZnO nanoparticles against microorganisms makes it an effective antimicrobial agent [7].

Conventional physical and chemical routes of synthesis of ZnO nanoparticles are expensive; require more labour, and huge space. Great amount of energy generated during the synthesis, raises the environmental temperature around the source material and disposal of large quantities of secondary waste is potentially toxic to all living beings [8]. Whereas biological route of synthesis of nanocomposite with aid of plants is a cost-effective eco-friendly method, with minimal expenditure and no adverse effects. Various phytochemical constituents present in a plant such as flavonoids, phenolics, terpenoids, polysaccharides, aldehydes, amines and proteins, act as reducing and stabilizing agents in the synthesis of nanoparticles [9]. *Strychnos nux-vomica* is an evergreen tree belonging to family Loganiaceae, mostly seen in an open habitat, native to Southeast Asia and India. It is cultivated commercially in different parts of the world such as United States, European Union, and throughout tropical Asia. It is a central nervous system stimulant; used for treatment of constipation and other stomach disorders, at a low-dose level. The plant is rich in bioactive chemicals, including alkaloids (such as strychnine and brucine) [10], flavonoids, tannins, saponins, and glycoside that aid in acting as (i) anti-inflammatory, (ii) anti-allergic, (iii) antioxidant, (iv) anti-diabetic, (v) antiviral, (vi) anti-cancer, (vii) analgesic, (viii) anti-spasmodic, and (ix) antibacterial agents [11].

Antimicrobial resistance remains a crucial issue to be considered in the efforts for organizing and resolving the treatment of non-healing infections, such as DFU [12]. Multidrug resistance has been reported in Gram-negative and Gram-positive bacteria such as *Pseudomonas aeruginosa*, *Acinetobacter* sps, *Enterobacteriaceae* sps, and *Staphylococcus aureus* due to diverse resistance mechanisms. These mechanisms include enzymatic degradation of antibiotics, reduced permeability, efflux pump mechanisms, and modification of bacterial proteins (the target for antibacterial) [13,14]. This necessitates the significance of alternative treatment strategies with much more efficiency than conventional antimicrobial agents to prevent plausible risk with dire financial consequences and life-threatening outcomes [15]. A few epidemiological studies have noted temporal changes in the frequency of resistance to a specific drug, when the amount of drug consumed in the community is deliberately reduced [16]. WHO has recently released the list of antibiotic-resistant "priority pathogens" of 12 bacterial families and has pointed out for the urgent need of the development of new antimicrobial agents [17]. Thence, the present study has investigated the green synthesis and characterization of ZnO nanocomposite of *Strychnos nux-vomica* L (Loganiaceae) leaf aqueous extract and evaluated the antimicrobial potency against MDR clinical and ATCC bacterial strains.

Material and methods

Materials

S. nux-vomica leaves were collected from forest areas of Western Ghats, South India, in June 2016. The plants were identified and authenticated by the Botanical Survey of India (Southern Circle), Coimbatore (BSC/SRC/5/23/2016/Tech/1197). The Zinc nitrate hexahydrate crystals [Zn $(NO_3)_2{\cdot}6H_2O$] of EMPLURA® grade was purchased from Merck (Darmstadt, Germany). The chemicals and glassware were procured from Sigma-Aldrich (St Louis, MO, USA) and Himedia (Mumbai, India). Multidrug-resistant clinical bacteria such as MRSA, *P. aeruginosa, A. baumannii,* and *E. coli* were isolated from the pus samples of DFU patients admitted at Rajah Muthiah Medical College and Hospital (RMMCH), India with the approval of Institutional Human Ethical Committee (M18/RMMC/2015). The patient samples were collected after obtaining informed consents from them. Preliminary identification and antibiotic susceptibility pattern of clinical isolates were processed at the Division of Microbiology, RMMCH. The results were further confirmed with VITEK 2® Compact automated system using GN Test Kit VTK2/GP Test Kit VTK2 (bio Mérieux, Marcy l'Etoile, France). The standard bacterial strains, *S. aureus* ATCC 29213, *P. aeruginosa* ATCC 27853, *E. faecalis* ATCC 29212, and *E. coli* ATCC 25922, were obtained from CSIR-National Chemical Laboratory, Pune, India.

Preparation of S. nux-vomica leaf aqueous extract

The leaves were washed thoroughly with double-distilled water and were allowed to dry at room temperature. Dried leaves were tattered and ground in a blender to a coarse powder. Plant powder (20 g) was heated with 100 mL of double-distilled water for 20 min at 60 °C. The light yellow coloured solution formed during boiling was allowed to cool to room temperature. In order to obtain a clear extract, the mixture was filtered through Whatman No.1 filter paper, centrifuged and stored in the refrigerator until further use.

Biosynthesis of S. nux-vomica–ZnO nanocomposite

Different concentrations of *S. nux-vomica* leaf aqueous extract (20, 30, and 40 mL) were added with 2 g of Zinc nitrate hexahydrate crystals and were allowed to dissolve using a magnetic stirrer. After complete dissolution of the mixture, the solution was vigorously stirred at 100 °C for 2 h until the colour changed from light yellow to deep yellow. After cooling at room temperature, the mixture was centrifuged at 5000 rpm for 10 min, and a solid precipitate was obtained. The solid product was centrifuged twice at 5000 rpm for 10 min after thorough washing and heated at 60–80 °C until the formation of deep yellow coloured paste. Annealing was carried out in a muffle furnace at 400 °C for 2 h. The light yellow coloured material obtained was ground using a mortar to a fine powder, which was used for further characterization and antibacterial assays.

Characterization studies of S. nux-vomica–ZnO nanocomposite

The XRD analysis (PANalytical Empyrean Alpha 1, Netherlands) was carried out using Cu Kα radiation (1.5406 Å) of a 2θ range of 20–80°; operating at 45 kV with a current of 30 mA to identify the structural information and crystalline phase. The average crystallite size was calculated using the Scherrer equation. Optical properties were analysed using UV–visible absorption spectroscopy (Varian Cary 5000, Palo Alto, California, USA). PL spectra of the samples were recorded using a fluorescence spectrometer (PerkinElmer LS55, Shelton, USA). Functional groups were identified using FTIR Spectrometer (Perkin Elmer-Spectrum Rx1, Shelton, USA) under identical conditions in the 400–4000 cm^{-1} region. The surface composition was analysed by XPS (AXIS-ULTRA, Kratos Analytical Ltd, UK). The morphology and size distribution of ZnO nanocomposite were characterized using HR-TEM with EDX (Jeol/JEM 2100, Tokyo, Japan) to confirm the presence of elemental zinc and oxygen. The data were analysed using Origin Pro 7.5 SRO software (OrginLab Corporation, USA).

Antibacterial assessment of S. nux-vomica–ZnO nanocomposite

The antibacterial activity of phytonanocomposite of ZnO was performed by the disc diffusion method [18] on Mueller-Hinton agar (MHA) as per the CLSI guidelines [19]. Whatman No.: 1 filter paper discs of 6-mm diameter were allowed to infuse with 200 and 400 μg/mL of ZnO phytonanocomposite dispersed in 20% dimethyl sulfoxide (DMSO) and kept at room temperature pending use. Bacterial suspensions were prepared in sterile saline (0.9% NaCl) by suspending overnight grown cultures on Columbia-based blood agar. The turbidity of bacterial suspension was adjusted to 0.5 McFarland standard and was evenly spread on MHA with a sterile cotton swab. Discs impregnated with ZnO phytonanocomposite, *S. nux-vomica* leaf aqueous extract, and bare ZnO nanoparticles were placed on inoculated MHA plates incubated at 37 °C. Control antibiotics, vancomycin (30 μg/mL) and colistin (10 μg/mL) were used as positive control for Gram-positive and negative bacteria, respectively, and the disc infused in 20% DMSO was used as a negative control. The plates were incubated at 37 °C for 24 h, the zone of inhibition of each well was measured, and the values were noted.

Statistical analysis

All the experiments were performed in triplicates, with the results being expressed as Mean ± Standard Deviation (SD) of three independent experiments. The means were statistically compared using One-way ANOVA followed by post hoc Dunnett's Multiple Comparison's tests using GraphPad Prism version 5. $P < .05$ was considered as statistically significant.

Results and discussion

XRD analysis of S. nux-vomica–ZnO nanocomposite

The XRD technique exploits the scattered intensity of an X-ray beam on the sample, thus providing information about the structural properties, physical, and chemical composition of the material studied. XRD pattern of ZnO phytonanocomposite synthesized from 20, 30, and 40 mL of *S. nux-vomica* leaf extract showed (Fig. 1) Bragg peaks corresponding well to (1 0 0), (0 0 2), (1 0 1), (1 0 2), (1 1 0), (1 0 3), (1 1 2), (2 0 1) and (2 0 2) *hkl* lattice planes of the hexagonal wurtzite structure (JCPDS Card no. 036-1451). Sharp and intense diffraction peaks indicated a high crystalline nature with a large particle size of bare ZnO nanoparticles [20]. However, in the case of ZnO phytonanocomposite, from different leaf extract volumes (20, 30, and 40 mL) exhibited an ascending pattern of broad and low-intensity diffraction peaks, indicating a reduced crystallite size with a faulting in its nanostructure [21]. Mean crystallite size was also calculated from XRD peaks using Debye–Scherrer formula, $D = 0.9\lambda/\beta \cos\theta$, where D is the average crystallite size, λ is the wavelength of X-ray, β is full width at half maximum in radians (FWHM), and θ is the Diffraction angle in radians. The obtained average particle size of ZnO phytonanocomposite was 31.18, 25.01, and 15.52 nm from 20, 30, and 40 mL of plant extract, respectively, and 69.85 nm for bare ZnO nanoparticles. XRD pattern of nanoparticles gave valuable structural information along with Debye–Scherrer calculation [22]. The above results clearly indicate that the optimal addition of plant extracts greatly influences the synthesis of ZnO nanocrystals with a reducing particle size. Various phytochemicals such as alkaloids, steroids, flavonoids, carbohydrates, glycosides, terpenoids, saponins, and proteins are acting as reducing and capping agents for the green synthesis of nanoparticles. This is in agreement with previous studies [23]. The concentration of leaf extract is effectively involved in controlling particle size when compared to bare ZnO nanoparticles.

Optical properties of S. nux-vomica–ZnO nanocomposite

UV–vis spectroscopy is a technique that is used to characterize optical properties of nanoparticles. The absorbance of ZnO phytonanocomposite synthesized from *S. nux-vomica* plant extract of 20, 30, and 40 mL shifted to smaller wavelengths of 351 nm, 341 nm, and 335 nm (Fig. 2a), respectively; the finding which is in line earlier report [24]. The absorbance of bare ZnO nanoparticles was approximately 353 nm (Fig. 2b). The wavelength of absorption spectrum below 358 nm, indicated a strong blue shift in absorption spectra due to reduced particle size, lesser than bulk excitation of the Bohr radius, in accordance to the previous literature [25]. The direct band gap energy of green biosynthesized ZnO phytonanocomposite was calculated by Wood-Tauc's relation [26]. It was estimated to be 3.53 eV, 3.64 eV, and 3.7 eV, corresponding to 351, 341, and 335 nm, respectively. Increased band gap (Eg) is the effect of quantum confinement on nano regime. Moreover, direct optical band gap energy (eV) is inversely proportional to the particle size of nanoparticles [27]. On the basis of XRD data and UV–visible-absorption spectrum, ZnO phytonanocomposite from 40 mL plant extract exhibited least particle size and high band gap energy (15.52 nm, 3.7 eV) than that of 30 mL (25.01 nm, 3.64 eV), and 20 mL (31.18 nm, 3.53 eV) of *S. nux-vomica* plant extract. Since the previous study [28] has pointed out the enhanced biological effects of nanoparticles with reduced crystallite size, ZnO phytonanocomposite prepared from 40 mL of *S. nux-vomica* plant extract was analysed for further studies.

PL provides valuable information regarding the purity and quality of the crystallite structures. PL spectra of ZnO phytonanocomposite synthesized from 40 mL of *S. nux-vomica* plant extract exhibited the emission peaks at 421.5, 443, 458.5, 482, and 528.5 nm (Fig. 3a). All the PL emission bands were in the visible light range, i.e., the deep level emission can be attributed to the structural defects of ZnO nanoparticles [29]. Emission peaks 421.5 and 443 nm in the range of violet–blue spectrum, indicated the presence of interstitial zinc (Zni). Blue–green emission at 458.5 and 482 nm can be ascribed to zinc vacancies (VZn). Green emission at 528.5 nm indicated singly ionized oxygen vacancies (VO) [30]. Thus, high-intensity PL emission bands in the range of the defect-oriented visible spectrum occurred due to faster and effective trapping of the photogenerated holes at the surface site, because of the high number of singly ionized oxygen vacancies and zinc vacancies. This indicates the presence of structural defects

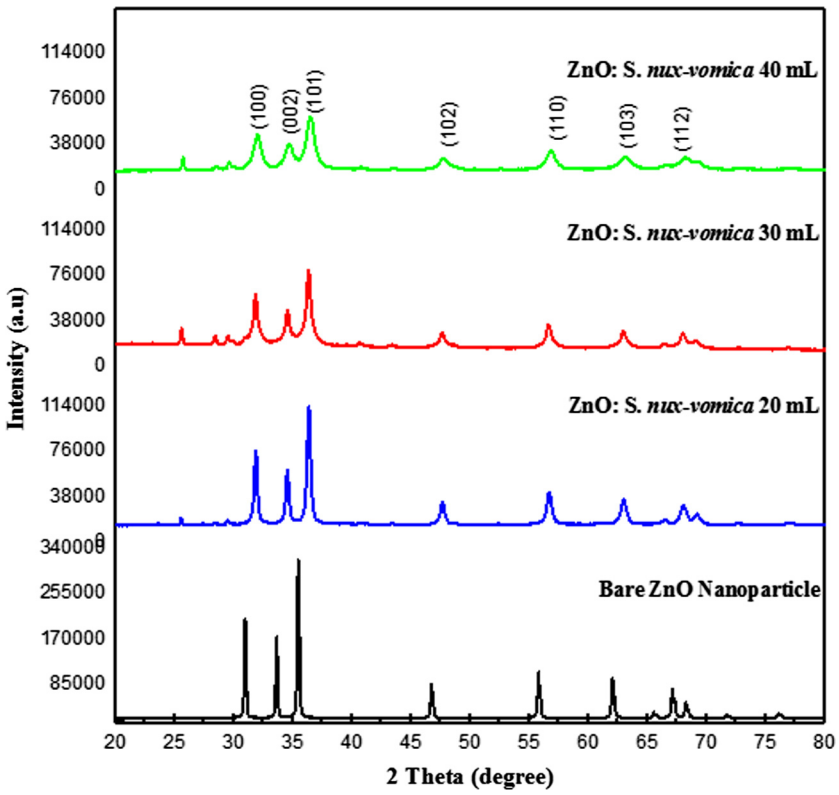

Fig. 1. XRD pattern of biosynthesized *S. nux-vomica*–ZnO nanocomposite.

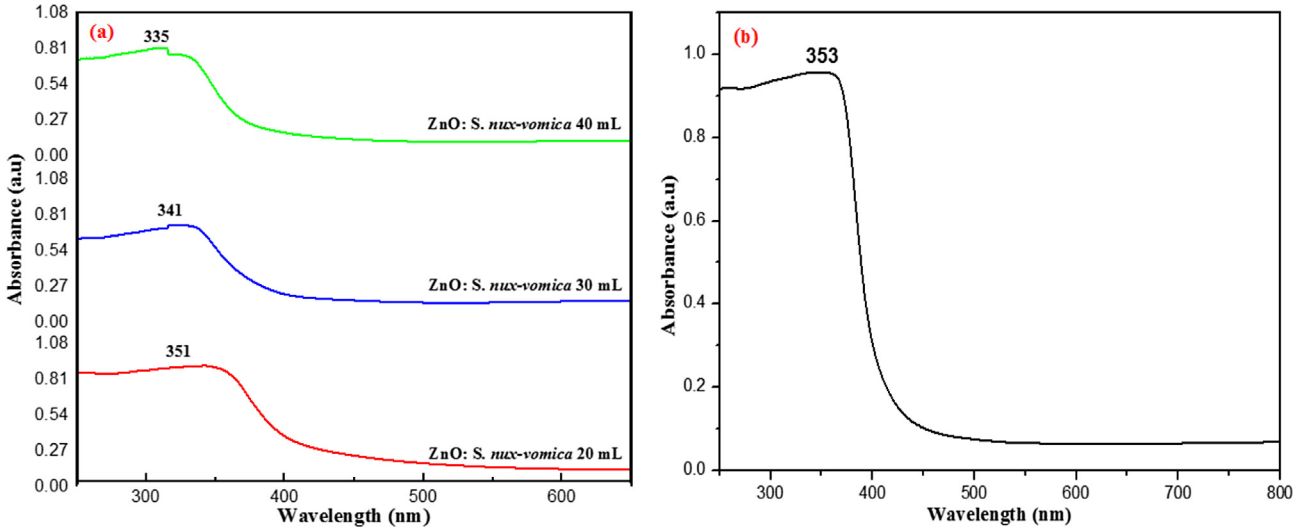

Fig. 2. UV–visible absorbance spectra of (a) biosynthesized *S. nux-vomica*–ZnO nanocomposite (b) bare ZnO nanoparticles at room temperature.

in ZnO nanocrystals, which may be responsible for its biological features [31]. Fig. 3b shows PL spectra for bare ZnO nanoparticles with low intense three emission bands (411, 461, and 480 nm) corresponding to broad deep-level (BDL) visible emissions, indicating zinc interstitial vacancies with low crystalline features.

FTIR analysis of S. nux-vomica–ZnO nanocomposite

The FTIR spectral analysis was conducted to identify the possible biomolecules responsible for the synthesis of *S. nux-vomica*–ZnO phytonanocomposite. FTIR spectra of *S. nux-vomica* plant extract (Fig. 4a) has shown broad absorption bands at 3280.92 cm^{-1}, representing OH stretching vibrations of water, alcohols, and phenols [25]. The weak absorption peak at 2927.94 cm^{-1} represented C—H stretching of alkanes and alkynes. The peak at 1589.34 cm^{-1} represented N—H bending vibrations of amines. Stretching vibrations present at 1394.53 cm^{-1} represented C═O stretching of alkanes and alkyls [24]; 1267.23 cm^{-1} were associated with C—N stretching vibrations of aliphatic amines [9]. Stretching vibrations of 1068.56 cm^{-1} and 1026.13 cm^{-1} represented C—O stretching of alcohols and carboxylic acid groups. The above data indicated the presence of phenols, terpenoids,

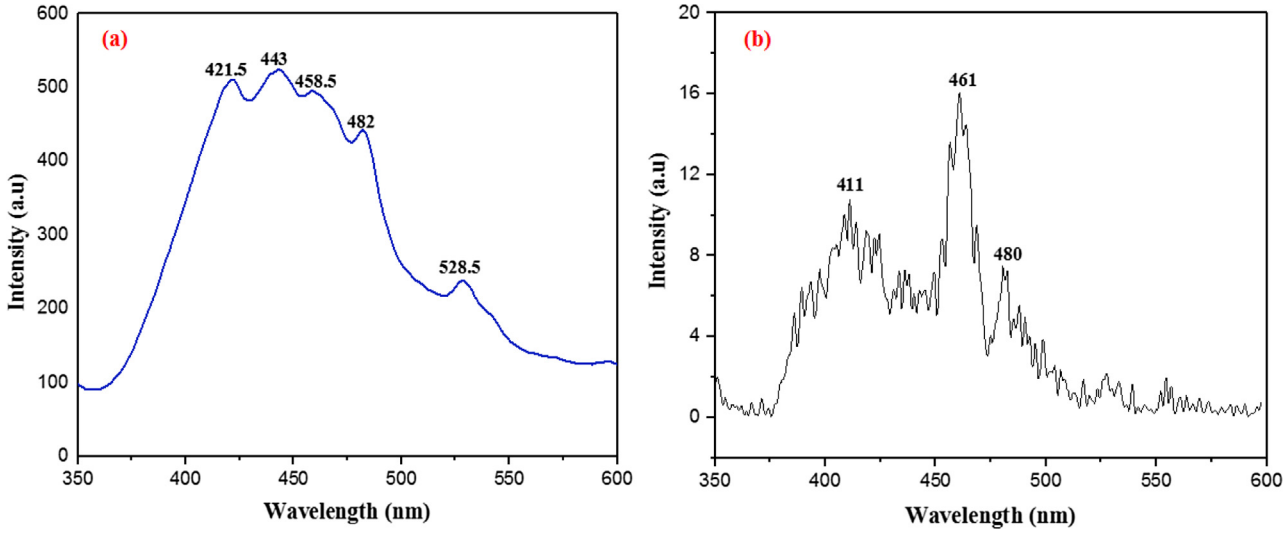

Fig. 3. Photoluminescence of (a) *S. nux-vomica*–ZnO nanocomposite in 40 mL (b) bare ZnO nanoparticles at room temperature.

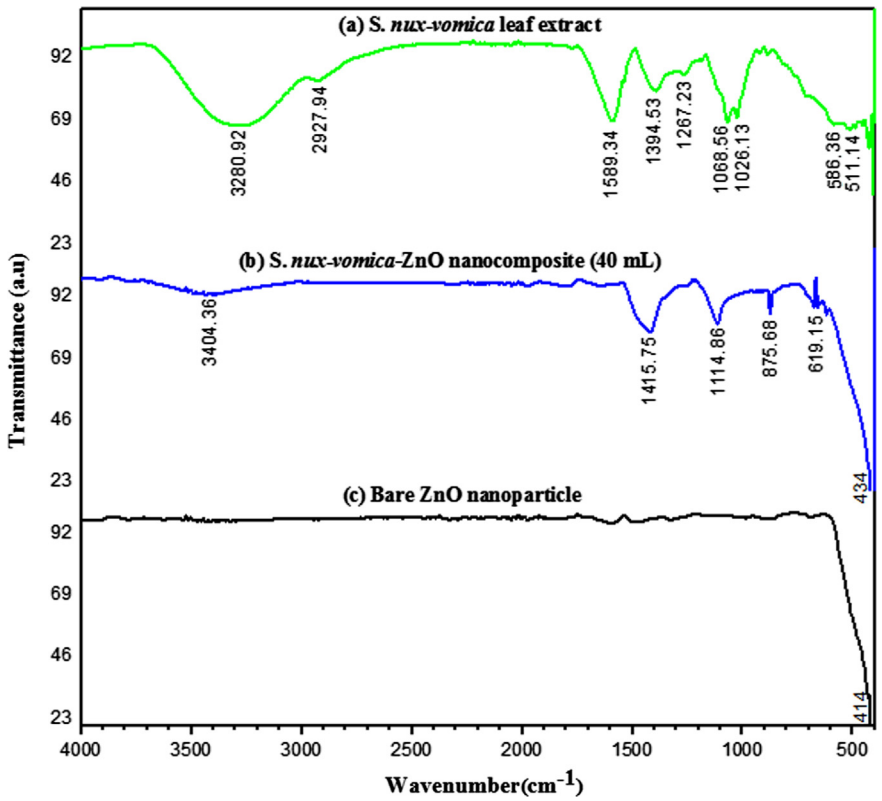

Fig. 4. FTIR spectra of (a) *S. nux-vomica* leaf aqueous extract (b) biosynthesized *S. nux-vomica*–ZnO nanocomposite in 40 mL (c) bare ZnO nanoparticles.

flavonoids, amino acids, carbohydrates, tannins, and saponins in *S. nux-vomica* plant extract [32]. FTIR spectra of ZnO phytonanocomposite from 40 mL of *S. nux-vomica* plant extract (Fig. 4b) exhibited an IR absorption band highly shifted 3280.92–3404.36, 1589.34–1415.75, 1267.23–1114.86, 1068.56–875.68, 586.36–619.15, and 511.14–434 cm^{-1}. This indicates the participation of soluble phytochemicals such as polyols, terpenoids, and proteins having functional groups of amines, alcohols, ketones and carboxylic acids, as reducing and stabilizing agents that aid in the formation of ZnO phytonanocomposite, preventing aggregation of nanoparticles in the solution [27]. The wide peak in the range of 530–420 cm^{-1} is characterized by zinc oxide and is associated with the stretching vibrations in Zn-O shown in the region of 434 cm^{-1} [33].

XPS analysis of S. nux-vomica–ZnO nanocomposite

The wurtzite nature and the chemical purity of the *S. nux-vomica*–ZnO nanocomposite were confirmed by XPS analysis. Wide scan of XPS spectra shown in Fig. 5a exhibited Zn and O peaks and hence sustained the chemical purity of the surface of *S. nux-vomica*–ZnO nanocomposite. Fig. 5b and c showed the high-resolution XPS spectra of the elements Zn and O, respectively.

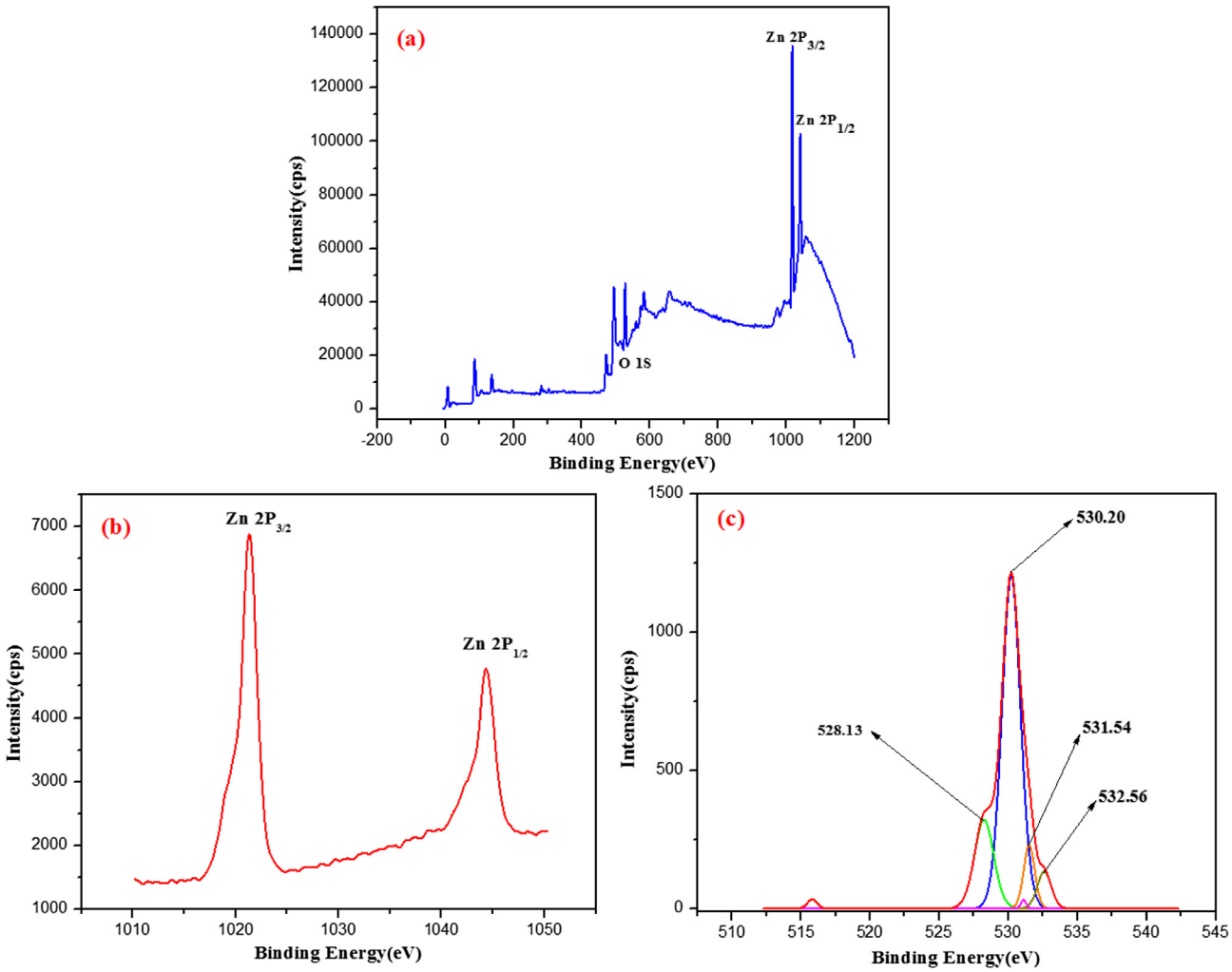

Fig. 5. XPS of biosynthesized *S. nux-vomica*–ZnO nanocomposite in 40 mL (a) wide range, (b) Zn, (c) O.

Two strong peaks centred at 1021.19 and 1044.15 eV corresponding to the Zn $2p_{3/2}$ and Zn $2p_{1/2}$ are clearly observed in Fig. 5b. These values are in concurrence with the binding energies of Zn^{2+} ion similar to the earlier reports [9]. The deconvolution of the O1s, which is ascribed to the O_2^- ions in the wurtzite ZnO structure, demonstrated four major peaks centred at 528.13, 530.20, 531.54, and 532.56 eV (Fig. 5c). According to a previous study, they originated from surface defects and chemisorbed oxygen, respectively [30].

TEM and EDX analysis of S. nux-vomica–ZnO nanocomposite

The transmission electron microscopic analysis was performed to study the morphology and size of the biosynthesized ZnO nanocrystals. TEM images of ZnO phytonanocomposite shown in Fig. 6a reported agglomerated quasi-spherical–shaped ZnO nanoparticles, with average size within a range of 10–20 nm. Particle size demonstrated in histogram data with a Gaussian distribution centred at ⟨φ particle⟩ is ~11.68 nm (Fig. 6b). The Selected Area Electron Diffraction (SAED) patterns shown in Fig. 6c is of combined spotty ring pattern; indicating that synthesized nanoparticles are of highly multi-crystalline nature. The HR-TEM image at resolution of 0.5 nm (Fig. 6d) has focussed on single ZnO phytonanocomposite, revealing its reticular plans at the distance between 0.25 nm and 0.26 nm, equivalent to d (Å) and corresponding to *hkl* lattice planes of (1 0 1) and (0 0 2) of zincite hexagonal wurtzite structure (JCPDS-36-1451). This correlated with XRD pattern of *S. nux-vomica–ZnO nanocomposite* in agreement with previous study [34]. EDX analysis of green synthesized ZnO phytonanocomposite using *S. nux-vomica* plant extract showed high-intensity peaks of Zn element and low-intensity peaks of O, Cl, K, Ca, and C elements (Fig. 7), which confirmed the presence of ZnO nanoparticles. The weak signals of other elements are due to presence of biometabolites in the plant extract, which is capped on the surface of ZnO phytonanocomposite [29].

Antibacterial assessment of S. nux-vomica–ZnO nanocomposite

The antibacterial activity of biosynthesized *S. nux-vomica*–ZnO nanocomposite towards standard bacterial strains and clinical bacterial isolates from DFU tested by standard disc diffusion on MHA are summarized in Table 1. Green synthesized ZnO phytonanocomposite exhibited significant antimicrobial activity against MDR clinical and ATCC bacterial strains, which was evaluated by a zone of inhibition in millimetre (mm). A maximum zone of inhibition was exhibited by *S. aureus* ATCC 29213 (22.33 ± 1.53 mm) and by MDR–MRSA (22.33 ± 1.16 mm), compared to plant extract and bare ZnO nanoparticles. A minimum zone of inhibition was observed against *E. faecalis* ATCC 29212 (about 12.33 ± 0.58 mm). However, green synthesized ZnO phytonanocomposite had more antibacterial potential than *S. nux-vomica* plant extract and bare ZnO nanoparticles. Enhanced antibacterial activity is due to the

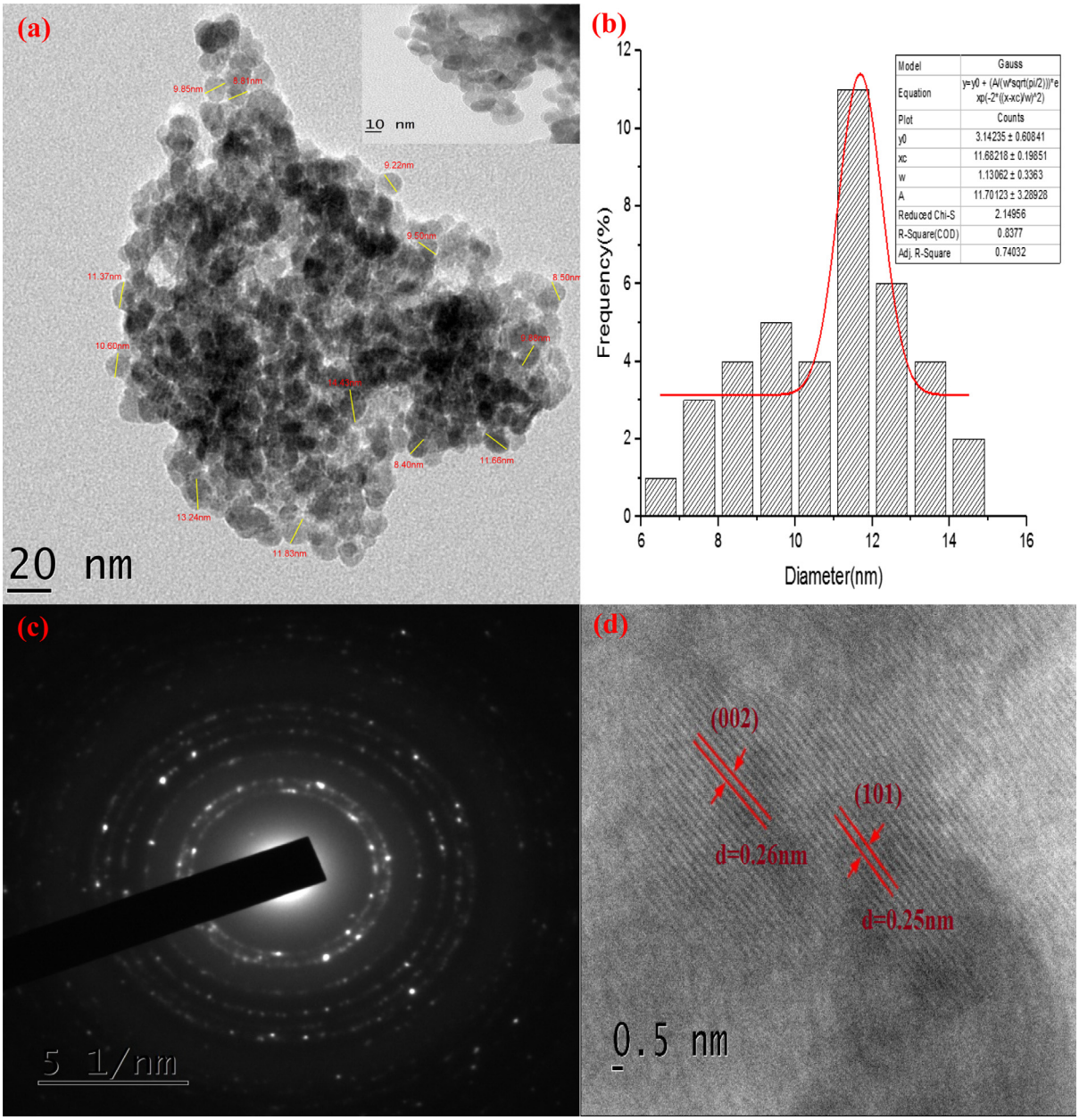

Fig. 6. TEM image of (a) annealed biosynthesized *S. nux-vomica*–ZnO nanocomposite in 40 mL inset picture of higher magnification, (b) gaussian distribution of particle size corresponding to TEM images, (c) selected area electron diffraction (SAED) pattern, (d) HR-TEM image.

presence of soluble phytochemicals responsible for the medicinal properties of *S. nux-vomica* leaf demonstrated through FTIR analysis, acting as a precursor for the green synthesis of ZnO phytonanocomposite. FTIR spectral data of *S. nux-vomica*–ZnO nanocomposite also showed the presence of functional compounds of phytochemical compounds even after annealing at 400 °C; proving the presence of plant compounds in ZnO phytonanocomposite, thus responsible for its antimicrobial effects (Fig. 4).

Gram-positive cocci including MDR–MRSA, and *S. aureus* ATCC 29213 exhibited higher antibacterial potential than Gram-negative bacteria, based on the results of disc diffusion assay on MHA. Increased susceptibility of Gram-positive bacteria over Gram-negative bacteria could be related to differences in cell wall structure, cell physiology, metabolism or degree of contact [35]. Lipopolysaccharide (LPS) present in the cell wall of Gram-negative bacteria may resist the bactericidal action of ZnO phytonanocomposite than Gram-positive bacteria devoid of LPS. Above results can be correlated with similar results to the study of Qian et al. [36] on green nano formulation of ZnO Aloe vera, which also demonstrated higher antibacterial efficiency of Gram-positive cocci, *S. aureus* (17.55 ± 0.02 to 28.12 ± 0.26 mm) than Gram-negative bacilli *E. coli* (15.38 ± 0.07 to 26.45 ± 0.08 mm).

Several mechanisms have been reported for the antibacterial activity of nanoparticles. The reduced particle size of ZnO phytonanocomposite demonstrated through XRD pattern and UV–visible-spectroscopy, resulted in remarkable increase in the surface area favouring the generation of free excitons, leading to the production of Reactive Oxygen species (ROS) lethal to bacterial cells. Uneven edges and surfaces of *S. nux-vomica*–ZnO nanocomposite demonstrated as surface defects in PL spectroscopy on contact with bacterial cells also cause damage to its bacterial cell membrane [37]. ZnO nanoparticles can interact with membrane lipids and disorganize the membrane structure, which leads to loss of membrane integrity, malfunction, and finally to bacterial death [38].

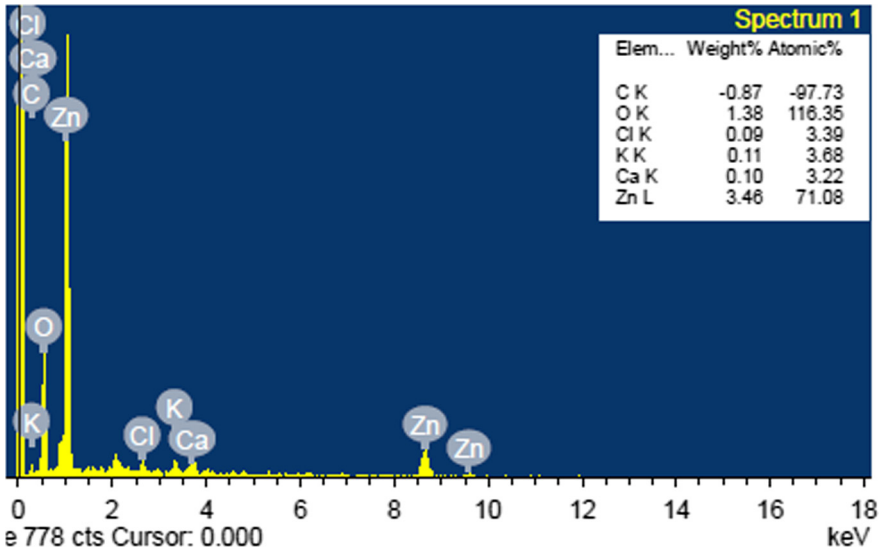

Fig. 7. EDX spectrum of biosynthesized *S. nux-vomica*–ZnO nanocomposite in 40 mL.

Table 1
Mean zone of inhibition (mm)[a] by disc diffusion[b] assay.

Name	*S. nux-vomica* C[c] (400 μg/mL)	Bare ZnO nano (400 μg/mL)	*S. nux-vomica* ZnO-nano (200 μg/mL)	*S. nux-vomica* ZnO-nano (400 μg/mL)	Control[d]	Antibiotic[e]
S. aureus ATCC 29213	7.33 ± 1.53	6.33 ± 0.58 ^{ns}	16.00 ± 1.00 ***	22.33 ± 1.53 ***	–	18.33 ± 0.58 ***
P. aeruginosa ATCC 27853	8.00 ± 1.00	6.33 ± 0.58 ^{ns}	9.67 ± 0.58 ^{ns}	16.00 ± 1.00 ***	–	12.67 ± 0.58 ***
E. faecalis ATCC 29212	8.00 ± 0.00	7.00 ± 1.00 ^{ns}	11.00 ± 1.00 **	12.33 ± 0.58 ***	–	18.00 ± 1.00 ***
E. coli ATCC 25922	7.00 ± 1.00	9.33 ± 0.58 ^{ns}	11.33 ± 0.58 ***	16.00 ± 1.00 ***	–	18.33 ± 0.58 ***
MDR–MRSA	7.33 ± 1.53	7.00 ± 0.00 ^{ns}	20.00 ± 1.00 ***	22.33 ± 1.16 ***	–	18.33 ± 0.58 ***
MDR–*P. aeruginosa*	7.00 ± 1.00	6.33 ± 0.58 ^{ns}	10.33 ± 0.58 **	13.33 ± 1.53 ***	–	12.67 ± 0.58 ***
MDR–*A. baumannii*	7.67 ± 0.58	7.00 ± 1.00 ^{ns}	8.00 ± 1.00 ^{ns}	13.00 ± 1.00 ***	–	11.00 ± 1.00 **
MDR–*E. coli*	7.00 ± 1.00	7.00 ± 1.00 ^{ns}	12.67 ± 0.58 ***	16.00 ± 1.00 ***	–	12.67 ± 0.58 ***

$^{*}P < .05$ in comparison with *S. nux-vomica* Crude. $P < .05$ was considered as statistically significant.
[a] Diameter zone of inhibition (mm) including the disc diameter of 6 mm.
[b] Mean ± SD of three independent experiments.
[c] *S. nux-vomica* crude extract.
[d] Negative control 20% DMSO.
[e] Antibiotic positive control Vancomycin 30 μg/mL for Gram-positive and Colistin 10 μg/mL for Gram-negative bacteria.
^{ns} Non significant.
*** $P < .001$.
** $P < .01$.

ZnO phytonanocomposite may also penetrate into bacterial cells at a nanoscale level and result in the production of toxic oxygen radicals, which damage DNA, cell membranes or cell proteins, and may finally lead to the inhibition of bacterial growth and eventually to bacterial cell death [39]. Kairyte et al. [40] has also demonstrated the antibacterial activity of ZnO nanoparticles due to electrostatic interaction within bacterial cell wall and also by the production of reactive oxygen species, eventually leading to the destruction of bacteria by cell shrinkage, degeneration of the membrane and surface of bacterial cells.

Conclusions

The present study demonstrated the biosynthesis of ZnO phytonanocomposite using *S. nux-vomica* leaf aqueous extract. Soluble phytochemicals of the plant enabled the synthesis of ZnO phytonanocomposite as reducing and stabilizing agents. On the basis of XRD patterns and UV–visible spectroscopy, particle size can be controlled by optimal addition of plant extract volume. Structural and surface properties of *S. nux-vomica*–ZnO nanocomposite enabled remarkable bactericidal activity against MDR bacterial isolates as well as ATCC bacterial strains demonstrated through disc diffusion on MHA. Thus, antimicrobial assays of biosynthesized ZnO phytonanocomposite against tested bacterial strains proved to have significant antibacterial activity and remarkable bactericidal properties against MDR bacterial isolates from DFU, also enlisted as critical and high prioritized pathogens by WHO. However, further studies are necessitated to understand the mechanism of bactericidal activity and possible toxicity.

Conflict of interest

The authors report no conflicts of interest in this work.

Compliance with Ethics Requirements

This article does not contain any studies with human or animal subjects.

Acknowledgement

The authors wish to acknowledge the financial support from DST-INSPIRE fellowship received by Ms. Katherin Steffy

(IF140576) under the guidance of Dr G. Shanthi. The authors also thank Professor and Head, Division of Microbiology, RMMC, and Professor and Head, Department of Pharmacy, Annamalai University, for providing necessary facilities to carry out this work. The authors cordially thank Sophisticated Analytical Instrument Facility, STIC, and CUSAT for recording HR-TEM and VIT University for Spectroscopy analysis.

References

[1] Gomez JL, Tigli O. Zinc oxide nanostructures: from growth to application. J Mater Sci 2013;48:612–24.
[2] Gao PX, Wang ZL. Substrate atomic-termination-induced anisotropic growth of ZnO nanowires/nanorods by the VLS process. J Phys Chem B 2004;108:7534–7.
[3] Djuriić AB, Ng AMC, Chen XY. ZnO nanostructures for optoelectronics: material properties and device applications. Prog Quantum Electron 2010;34:191–259.
[4] Carcia PF, McLean RS, Reilly MH, Crawford MK, Blanchard EN, Kattamis AZ, et al. A comparison of zinc oxide thin-film transistors on silicon oxide and silicon nitride gate dielectrics. J Appl Phys 2007;102:074512.
[5] Gordon RG. Criteria for choosing transparent conductors. MRS Bull 2000;25:52–7.
[6] Salem W, Leitner DR, Zingl FG, Schratter G, Prassl R, Goessler W, et al. Antibacterial activity of silver and zinc nanoparticles against *Vibrio cholerae* and enterotoxic *Escherichia coli*. Int J Med Microbiol 2015;305:85–95.
[7] Premanathan M, Karthikeyan K, Jeyasubramanian K, Manivannan G. Selective toxicity of ZnO nanoparticles toward Gram-positive bacteria and cancer cells by apoptosis through lipid peroxidation. Nanomed Nanotechnol, Biol Med 2011;7:184–92.
[8] Kruis FE, Fissan H, Rellinghaus B. Sintering and evaporation characteristics of gas-phase synthesis of size-selected PbS nanoparticles. Mater Sci Eng B 2000; B69:329–34.
[9] Ramesh M, Anbuvannan M, Viruthagiri G. Green synthesis of ZnO nanoparticles using *Solanum nigrum* leaf extract and their antibacterial activity. Spectrochim Acta – Part A Mol Biomol Spectrosc 2015;136:864–70.
[10] Deng X, Yin W, Li W, Yin F, Lu X, Zhang X, et al. The anti-tumor effects of alkaloids from the seeds of *Strychnos nux-vomica* on HepG2 cells and its possible mechanism. J Ethnopharmacol 2006;106:179–86.
[11] Patel DK, Patel K, Duraiswamy B, Dhanabal SP. Phytochemical analysis and standardization of *Strychnos nux-vomica* extract through HPTLC techniques. Asian Pacific J Trop Dis 2012;2:S56–60.
[12] Katiyar C, Kumar A, Bhattacharya SK, Singh RS. Ayurvedic processed seeds of *nux-vomica*: neuropharmacological and chemical evaluation. Fitoterapia 2010;81:190–5.
[13] Armstrong DG, Lavery LA, Wrobel JS, Vileikyte L. Quality of life in healing diabetic wounds: does the end justify the means? J Foot Ankle Surg 2008;47:278–82.
[14] Kumar VA, Steffy K, Chatterjee M, Sugumar M, Dinesh KR, Manoharan A, et al. Detection of oxacillin-susceptible mecA-positive *Staphylococcus aureus* isolates by use of chromogenic medium MRSA ID. J Clin Microbiol 2013;51:318–9.
[15] Hobizal KB, Wukich DK. Diabetic foot infections: current concept review. Diabet Foot Ankle 2012;1:1–9.
[16] Johnsen PJ, Townsend JP, Bohn T, Simonsen GS, Nielsen KM. Factors affecting the reversal of antimicrobial-drug resistance. Lancet 2009;9:357–64.
[17] WHO publishes list of bacteria for which new antibiotics are urgently needed, (World Health Organization, 2017) <http://www.who.int/mediacentre/news/releases/2017/bacteria antibiotics-needed/en/2017> [accessed 03.03.2017].
[18] Bauer AW, Kirby WMM, Sherris JC, Turk M. Antibiotic susceptibility testing by standard single disk method. Am J Clin Pathol 1966;45:493–6.
[19] Clinical and Labortaory Standard Institute (CLSI), Performance standards for antimicrobial susceptibility testing: twenty-fifth informational supplement (M100–S25) Wayne PA; 2015.
[20] Azizi S, Ahmad MB, Namvar F, Mohamad R. Green biosynthesis and characterization of zinc oxide nanoparticles using brown marine macroalga *Sargassum muticum* aqueous extract. Mater Lett 2014;116:275–7.
[21] Suresh D, Shobharani RM, Nethravathi PC, Pavan Kumar MA, Nagabhushana H, Sharma SC. *Artocarpus gomezianus* aided green synthesis of ZnO nanoparticles: luminescence, photocatalytic and antioxidant properties. Spectrochim Acta – Part A Mol Biomol Spectrosc 2015;141:128–34.
[22] Abdel-Hameed SAM, Marzouk MA, Farag MM. Effect of P_2O_5 and MnO_2 on crystallization of magnetic glass ceramics. J Adv Res 2014;5:543–50.
[23] Fatimah I. Green synthesis of silver nanoparticles using extract of *Parkia speciosa Hassk* pods assisted by microwave irradiation. J Adv Res 2016;7:961–9.
[24] Anbuvannan M, Ramesh M, Viruthagiri G, Shanmugam N. *Anisochilus carnosus* leaf extract mediated synthesis of zinc oxide nanoparticles for antibacterial and photocatalytic activities. Mater Sci Semicond Process 2015;39:621–8.
[25] Ambika S, Sundrarajan M. Plant-extract mediated synthesis of ZnO nanoparticles using *Pongamia pinnata* and their activity against pathogenic bacteria. Adv Powder Technol 2015;26:1294–9.
[26] Steffy K, Shanthi G, Maroky AS, Selvakumar S. Enhanced antibacterial effects of green synthesized ZnO NPs using *Aristolochia indica* against Multi-drug resistant bacterial pathogens from Diabetic Foot Ulcer. J Infect Public Health 2017. doi: https://doi.org/10.1016/j.jiph.2017.10.006.
[27] Bhuyan T, Mishra K, Khanuja M, Prasad R. Biosynthesis of zinc oxide nanoparticles from *Azadirachta indica* for antibacterial and photocatalytic applications. Mater Sci Semicond Process 2015;32:55–61.
[28] Yamamoto O. Influence of particle size on the antibacterial activity of zinc oxide. Int J Inorg Mater 2001;3:643–6.
[29] Elumalai K, Velmurugan S, Ravi S, Kathiravan V, Ashokkumar S. Bio-fabrication of zinc oxide nanoparticles using leaf extract of curry leaf (*Murraya koenigii*) and its antimicrobial activities. Mater Sci Semicond Process 2015;34:365–72.
[30] Diallo A, Ngom BD, Park E, Maaza M. Green synthesis of ZnO nanoparticles by *Aspalathus linearis*: structural and optical properties. J Alloy Compd 2015;646:425–30.
[31] Mo CM, Li YH, Liu YS, Zhang Y, Zhang LD. Enhancement effect of photoluminescence in assemblies of nano-ZnO particles/silica aerogels. J Appl Phys 1998;83:4389–91.
[32] Suresh S, Karthikeyan S, Jayamoorthy K. Effect of bulk and nano-Fe_2O_3 particles on peanut plant leaves studied by Fourier transform infrared spectral studies. J Adv Res 2016;7:739–47.
[33] Nagarajan S, Kuppusamy AK. Extracellular synthesis of zinc oxide nanoparticle using seaweeds of gulf of Mannar, India. J Nanobiotechnol 2013;11:39.
[34] Thema FT, Manikandan E, Dhlamini MS, Maaza M. Green synthesis of ZnO nanoparticles via *Agathosma betulina* natural extract. Mater Lett 2015;161:124–7.
[35] Reddy KM, Feris K, Bell J, Wingett DG, Hanley C, Punnoose A. Selective toxicity of zinc oxide nanoparticles to prokaryotic and eukaryotic systems. Appl Phys Lett 2007;90:1–3.
[36] Qian Y, Yao J, Russel M, Chen K, Wang X. Characterization of green synthesized nano-formulation (ZnO-*A. vera*) and their antibacterial activity against pathogens. Environ Toxicol Pharmacol 2015;39:736–46.
[37] Padmavathy N, Vijayaraghavan R. Enhanced bioactivity of ZnO nanoparticles—an antimicrobial study. Sci Technol Adv Mat 2008;9:1–7.
[38] Xiu Z, Zhang Q, Puppala HL, Colvin VL, Alvarez PJJ. Negligible particle-specific antibacterial activity of silver nanoparticles. Nano Lett 2012;12:4271–5.
[39] Lipovsky A, Tzitrinovich Z, Friedmann H, Applerot G, Gedanken A, Lubart R. EPR study of visible light-induced ROS generation by nanoparticles of ZnO. J Phys Chem C 2009;113:15997–6001.
[40] Kairyte K, Kadys A, Luksiene Z. Antibacterial and antifungal activity of photoactivated ZnO nanoparticles in suspension. J Photochem Photobiol B Biol 2013;128:78–84.